

Late Pleistocene landscape response to climate change: eolian and alluvial fan deposition, Cape Liptrap, southeastern Australia

Thomas W. Gardner^{a,*}, John Webb^b, Aaron G. Davis^a, Elizabeth J. Cassel^a,
Claudia Pezzia^a, Dorothy J. Merritts^a, Barton Smith^{c,1}

^a*Keck Geology Consortium, The College of Wooster, 1189 Beall Avenue, Wooster, OH 44691, USA*

^b*Environmental Geoscience, La Trobe University, Victoria 3086, Australia*

^c*School of Earth Sciences, Melbourne University, Victoria 3010, Australia*

Received 31 March 2005; accepted 7 December 2005

Abstract

Sea cliffs along the western coast of Cape Liptrap at Arch Rock provide nearly continuous exposure of calcareous eolianites dated at 68–112 ka (five optically stimulated luminescence (OSL) ages). Calcareous eolian deposition began immediately after the last interglacial marine highstand (Oxygen Isotope Stage (OIS) 5e) and continued during sea level fall until the beginning of OIS 4. West-southwesterly winds transported calcareous sand across ~12 km of exposed continental shelf by the beginning of OIS 4. A brief period of cold, arid, windy continental climate with ephemeral, but intense, surface runoff immediately preceded the Last Glacial Maximum (LGM). This resulted in fluvial reworking of the calcarenites into an alluvial fan dated at 23–25 ka (four OSL ages). The fan overlies peat dated at 25,279 yr cal BP and is capped by a paleosol dated at 6010 yr cal BP. Concurrent eolian reworking by northwesterly winds of siliceous sediments on marine terraces along the eastern and central portion of Cape Liptrap formed siliceous longitudinal dunes with ages ranging from 19 to 24 ka (five OSL ages). The phase of maximum landscape instability at Cape Liptrap coincides with solar insolation and air temperature minima and preceded the LGM by several thousand years.

© 2006 Elsevier Ltd. All rights reserved.

1. Introduction

Pleistocene eolian deposits along the southeastern coast of Australia provide an unsurpassed record of glacial and interglacial atmospheric circulation patterns (Bowler, 1976, 1982; Sprigg, 1979; Hill and Bowler, 1995), climates (Bowler, 1976, 1990; Bowler, 1982; Sigleo and Colhoun, 1982; Nanson et al., 1992), eustatic sea levels (Blackburn, 1962; Boutakoff, 1963; Kenley, 1971; Cook et al., 1977; Sprigg, 1979; Jenkin, 1981; Murray-Wallace et al., 1999; Murray-Wallace et al., 2001) and uplift (Kenley, 1976; Sprigg, 1979; Sandiford, 2003). These deposits have been thoroughly described for many parts of the southeastern

coast (Fig. 1A) from South Australia (Boutakoff, 1963; Sprigg, 1979; Spiers, 1992; Zhou et al., 1994; Huntley et al., 1993; Oyston, 1996), Victoria (Jenkin, 1968, 1981; Jenkin et al., 1988; Hill and Bowler, 1995), New South Wales (Thom et al., 1994), Lord Howe Island (Price et al., 2001; Brooke et al., 2003) and Tasmania (Sigleo and Colhoun, 1982; Bowden, 1983). In general, they are divided into either a calcareous facies, commonly referred to as dune limestone or eolianite, or a siliceous facies. The calcareous eolian deposits are related to eustatic sea level maxima (Sprigg, 1979; Jenkin, 1981; Murray-Wallace et al., 1999; Murray-Wallace et al., 2001), but siliceous eolian deposits reflect increasing aridity, decreasing vegetation cover and changes in large-scale atmospheric circulation patterns (King, 1960; Bowler, 1976, 1982; Sprigg, 1979; Nanson et al., 1992; Thom et al., 1994; Hill and Bowler, 1995). All are ultimately controlled by Quaternary climate change, specifically glacial/interglacial cycles.

*Corresponding author. Department of Geosciences, Trinity University, One Trinity Place, San Antonio, TX 78212, USA.
Tel.: +1 210 999 7655; fax: +1 210 999 7090.

E-mail address: tgardner@trinity.edu (T.W. Gardner).

¹Current address: 33 Selkirk Street, North Perth 6006, Western Australia.

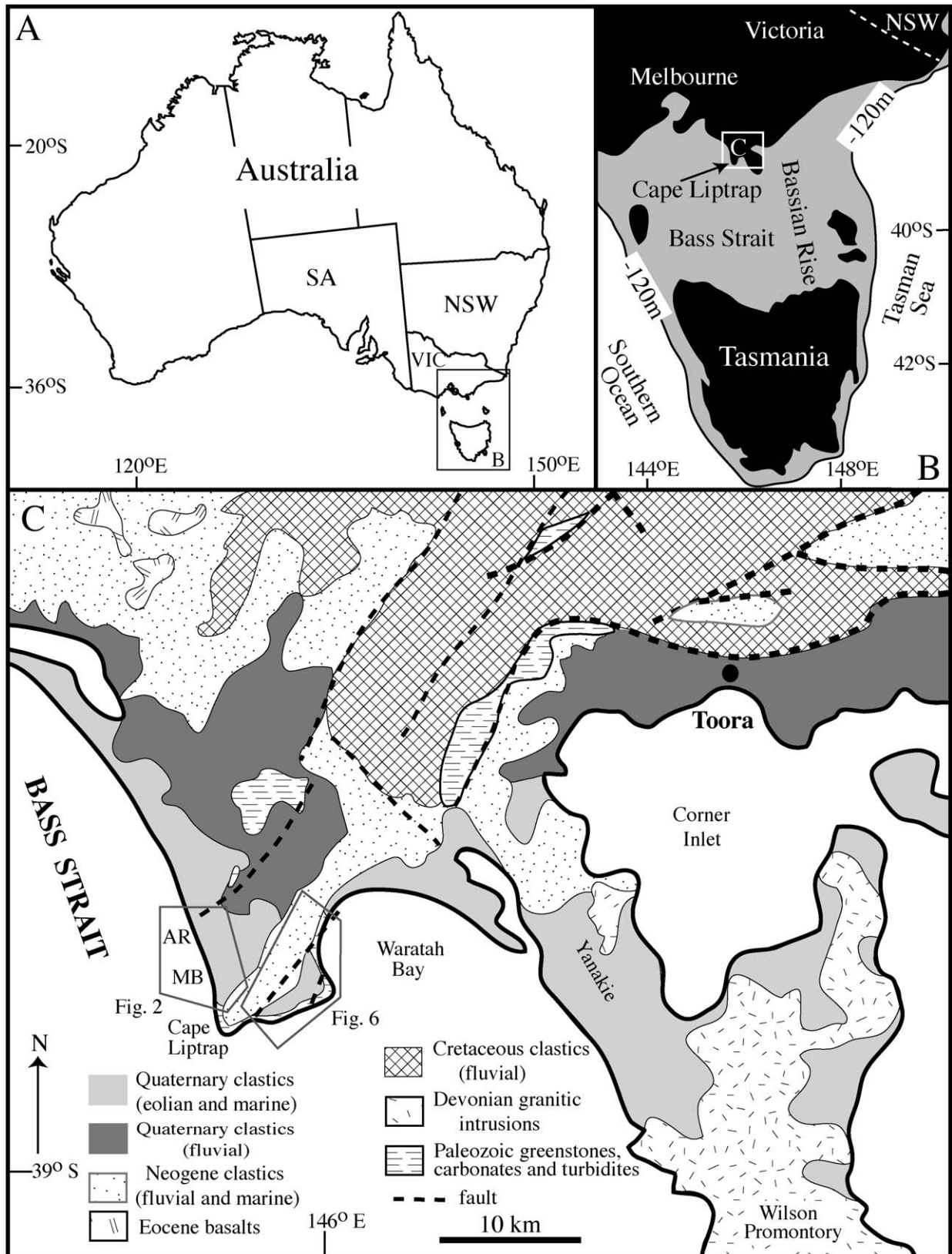


Fig. 1. (A) General setting of Australia; NSW, New South Wales; SA, South Australia, VIC, Victoria. (B) Location of Cape Liptrap relative to Tasmania and Melbourne; sea floor above -120m contour shaded in light grey; land in black. (C) Generalized geologic map for Cape Liptrap and Wilson Promontory; AR, Arch Rock; MB, Morgan Beach. Modified from Vandenberg (1997) and Douglas (1975). Polygonal boxes show location of calcareous eolianites at Arch Rock and alluvial fan at Morgan Beach (Fig. 2) and siliceous dunes on the eastern side of Cape Liptrap (Fig. 6).

The coastal dune systems of the Cape Liptrap area in southeastern Australia offer an excellent opportunity to better understand the Late Pleistocene landscape evolution, climates and atmospheric circulation patterns of this region for three compelling reasons. First, Cape Liptrap sits astride the boundary between predominantly calcareous coastal dunes to the west and mostly siliceous coastal dunes to the east. West of Cape Liptrap, the coastal dunes are predominantly calcareous sands, consisting of quartz and bryozoan and shell fragments originally derived from the bryozoan banks on the seafloor of Bass Strait and swept onto the beaches by the southwesterly ocean swell (Bird, 1961; Jenkin, 1981; Joyce et al., 2003) and eastward littoral drift (Baker, 1956). In contrast, east of Cape Liptrap, the siliceous sands consist predominantly of quartz derived from weathering of nearby granite and Paleozoic basement rocks. Here the coastal zone has a predominantly south-easterly ocean swell (Bird, 1961; Jenkin, 1981; Jenkin, 1988), and seasonally eastward or westward littoral drift (Jenkin, 1988). Second, the bathymetry of the continental shelf along this section of the southeastern Australian coast allows for over 250 km of migration of the coastline during glacial/interglacial stages (Fig. 1B). Given the pronounced, modern continental gradient in temperature and rainfall, this coastline shift optimizes the change from a temperate, maritime interglacial climate to an arid, continental glacial climate. Third, the Cape Liptrap area is the southernmost extension of the Australian mainland, extending just beyond 39° S. Together with Wilson Promontory, Tasmania and the offshore islands (Fig. 1B and C), Cape Liptrap affords a unique view of the southernmost climate and atmospheric circulation patterns associated with Quaternary climate changes in Australia.

In this paper, we describe well-exposed calcareous and siliceous eolian deposits at Cape Liptrap (Fig. 1C) and an alluvial fan deposit that was derived from the eolianites. From detailed stratigraphic descriptions, optically stimulated luminescence (OSL) ages, and radiocarbon ages, we infer environments of deposition and timing of the phase of maximum landscape instability. We speculate on global climate forcing of Last Glacial Maximum (LGM) climates and atmospheric circulation for southeastern coastal Australia.

2. Regional setting

Cape Liptrap lies astride the Bassian Rise, a broad platform on the Australian continental margin that extends south to Tasmania (Jenkin, 1981; Bowden, 1983; Hill and Bowler, 1995; Fig. 1A and B). Lower to Middle Paleozoic greenstones and limestones and Early Devonian turbidites of the Liptrap Formation are exposed in coastal outcrops and stream valleys on Cape Liptrap (Fig. 1C). Neogene and Quaternary marine, fluvial and eolian deposits of variable thickness cover most of the Palaeozoic bedrock. The Cape Liptrap Peninsula extends nearly 10 km southward from the coast, averages about 8 km in width, and is

dominated by a northeast-trending ridge with a maximum elevation of 170 m in the middle of the peninsula.

The climate is temperate marine with a mean annual temperature of $\sim 14^\circ\text{C}$, mean annual rainfall of $\sim 1\text{ m}$, and average 3 PM wind speed of $\sim 30\text{ km/h}$, with gusts exceeding 150 km/h recorded several times per year. Winds are predominantly from the west-southwest, but strong easterlies occur 10–20% of the time from November to March (Bureau of Meteorology, 2004). Where not cleared for agriculture, the coastal zone is a *Leptospermum*, *Melaleuca*, *Casuarina*-dominated shrubland, while inland forests consist predominantly of *Eucalyptus*, *Banksia* and *Casuarina* (Hope, 1974).

3. Site descriptions

Three separate locations were studied at Cape Liptrap: calcareous eolianites at Arch Rock, an alluvial fan at Morgan Beach, and siliceous dunes on the central and eastern part of the Cape Liptrap peninsula (Fig. 1C). At each location we measured detailed stratigraphic columns, cross-bedding dip direction for paleowind and paleocurrent analysis, and collected samples for petrographic and palynological analyses, OSL dating, and radiocarbon dating. We report first on the details of the OSL technique and results. We follow that with detailed stratigraphic descriptions of the eolianite, interbedded paleosols, alluvial fan, buried peat and the siliceous dunes.

4. OSL analysis

Sixteen samples (Table 1) were prepared for optical luminescence dating using the standard procedures of Galbraith et al. (1999). Luminescence measurements were made using Thorn-EMI 9235QA or 9235QB photomultiplier tubes with U-340 filters attached. A TL-DA-12 Risø OSL reader (Bøtter-Jensen and Duller, 1992) was used to analyze samples TG1, 2, 3, 4, 5, 8, 12, 14, and 16, which were stimulated using filtered 420–550 nm tungsten-halogen light delivered at a rate of $\sim 25\text{ mW/cm}^2$ at 125°C . The remaining samples were stimulated using a blue 470 nm LED array delivered at a rate of $\sim 25\text{ mW/cm}^2$ using a TL-DA-15 Risø reader (Bøtter-Jensen et al., 2000). Calibrated ^{90}Sr sources attached to the Risø sets were used for beta irradiations.

A single-aliquot-regenerative (SAR) procedure similar to that described by Murray and Wintle (2000) was applied to aliquots each containing ~ 300 grains. The first 0.4 s of OSL decay was integrated to estimate the signal count and the final 10 s to estimate the late light level. SAR dose–response curves were constructed using the program “Analyst” (Duller, 1999) until the D_E estimate was bracketed by successive regenerative doses. These curves included a 0 Gy regenerative dose to monitor recuperation. An initial IR shine of 25 s was employed to test for the presence of feldspar grains not eliminated by the chemical treatment. Each sample was analysed using a range of pre-heat

Table 1
Equivalent dose (D_E), dose rates, and luminescence ages for samples at Cape Liptrap

Sample ID ^a	Depth (m)	Equivalent dose (Gy)		K-series ^b	Th-series ^b	Ra-228	U-series ^b	Ra-226	Pb-210	K ^c	Th ^c	U ^c	Cosmic-ray dose-rate ^d	Total dose-rate (Gy/ka)		Age (ka)	
		K-40	Th-228											CSIRO	INAA	CSIRO	INAA
TG1	13.0	53±3.0								149±2	5.3±0.1	9±0.2	0.07±0.02	0.78±0.08		68±7	
TG2	21.0	54±3.0								111±2	6.7±0.1	6.9±0.2	0.07±0.02	0.66±0.07		83±8	
TG3	34.0	67±4.0	131.2±3.2	6.1±0.2	6.4±0.3	16.6±3.0	9.7±0.2	11.1±1.5		151±2	7.6±0.1	9.8±0.2	0.07±0.02	0.84±0.08	0.79±0.08	81±8	85±8.5
TG4	32.0	63±4.0								123±2	6.4±0.1	8.6±0.2	0.07±0.02	0.72±0.07		89±9	
TG5	1.1	18±1.6								142±2	6.6±0.1	5.4±0.3	0.13±0.02	0.78±0.08		23±2	
TG6	14.5	18±1.9	130.6±3.1	6.0±0.2	5.9±0.4	8.6±2.7	7.0±0.2	7.2±1.5		139±2	5.8±0.1	5.3±0.3	0.13±0.02	0.75±0.08	0.77±0.08	24±2	23±2.3
TG7	11.1	21±2.1								146±2	7±0.1	6.4±0.2	0.13±0.02	0.81±0.08		25±3	
TG8	12.9	19±2.0								163±3	7.7±0.1	4.7±0.3	0.11±0.02	0.83±0.08		23±2	
TG10	2.4	16±1.7	115.7±3.1	6.0±0.3	5.1±0.4	3.7±3.1	4.7±0.2	4.6±1.4		153±3	6.4±0.1	5.3±0.3	0.15±0.02	0.82±0.08	0.68±0.07	20±2	23±2.3
TG11	2.2	17±1.7								115±2	12±0.1	4.6±0.3	0.17±0.02	0.82±0.08		20±2	
TG12	1.3	14±1.5								91±2	5.3±0.1	3.5±0.4	0.18±0.02	0.62±0.06		22±2	
TG13	1.9	15±1.5	89.8±2.7	5.4±0.3	4.6±0.4	1.2±3.1	6.3±0.2	5.1±1.3		111±2	7.5±0.1	3.1±0.4	0.18±0.02	0.71±0.07	0.62±0.06	21±2	24±2.4
TG14	1.5	15±1.6								132±2	7.2±0.1	4.2±0.3	0.18±0.02	0.79±0.08		19±2	
TG16	2.1	17±1.8	128.5±3.9	21.1±0.5	19.8±0.6	11.5±4.4	19.0±0.4	15.5±2.2		140±2	14±0.1	3.7±0.4	0.18±0.02	0.91±0.09	1.26±0.13	19±2	12±1.2
AR01	1.5	75±6								105±2	5±0.1	4.5±0.4	0.16±0.02	0.67±0.04		112±11	
MB01	20.2	68±3.0	107.3±2.3	10.0±0.2	9.8±0.2	10.0±0.5	8.0±0.2	8.8±0.6					0.02±0.01	0.56±0.03		122±9.0	

^aFor all samples we assume a specific gravity of 2.7 g/cm³, porosity of 35%, and average field water content during burial of 5±2.5% (except the marine terrace sand, MB01, with an assumed water content of 25±5%).

^bActivity concentration of selected daughter products of the U and Th chains and K were measured using a high-resolution gamma-ray detector (Olley et al., 1996) at Commonwealth Scientific & Industrial Research Organization (CSIRO), Canberra. Values are in Bq/kg. The internal alpha dose-rate for all samples was assumed to be 0.025±0.01 Gy/ka.

^cK, U and Th concentrations of all samples were determined via Induced Neutron Activation Analysis (INAA) by Bequerel Laboratories (converted to Bq/kg using the conversion factors of Adamiec and Aitken (1998)).

^dCosmic-ray dose rates were calculated following Prescott and Hutton (1994).

temperatures (180–280 °C) to test for D_E dependency on pre-heat temperature. Routine tests of the repeatability of SAR cycles were also carried out using known laboratory doses.

For all samples the recuperated OSL and IR stimulated OSL were negligible, and the mean value ($n = 24$) of SAR repeatability overlapped with unity. The SAR cycle repeatability of a few individual aliquots did not overlap with unity and these aliquots were not used in the final D_E calculation. SAR cycle repeatability and D_E estimates were effectively independent of pre-heat temperature for all samples. SAR D_E estimates and their errors were calculated using the program “Analyst” supplied by Risø Laboratories.

All samples demonstrated adequate recovery of a known dose using the methods of Roberts et al. (1999). All group median equivalent doses and most individual aliquot equivalent doses were within $\pm 5\%$ of the known dose, and no aliquot was more than $\sim \pm 10\%$ from the known dose.

Equivalent dose, dose-rate, and luminescence ages are listed in Table 1. Sub-samples of TG3, 6, 10, 13, and 16 were ground, cast in resin discs, and set aside for 30 days to allow radon gas to equilibrate with its daughter products within the sediment/resin mixture. Where high-resolution gamma spectrometry data were obtained, these data were used instead of the INAA data in the age equation because the activity of more than one radionuclide in each of the U and Th decay series was measured, and because a larger sample mass was measured in the former. Where the ^{210}Pb concentration was found to be in deficit with respect to ^{226}Ra (samples TG13, and TG16), individual activity concentrations were factored separately into the dose-rate calculation to account for probable loss of ^{222}Rn gas to the atmosphere. Further, there is evidence for U-series disequilibria between the parent radionuclide ^{238}U and its daughter product, ^{226}Ra , in sample TG3. As a precaution, all U-series radionuclides have been factored separately into the dose-rate equation for this sample. Doing so increases the overall dose-rate for this sample by only 4% compared with using a weighted average of the activities because the K decay series makes up the majority of the total dose-rate.

5. Arch rock eolianites

5.1. Stratigraphy and sedimentology

For nearly 2 km along the western coast of Cape Liptrap at Arch Rock (Fig. 2), nine overlapping, calcareous eolianites with eight interbedded paleosols (Fig. 3A and E) outcrop along nearly continuous, 40 m high sea cliffs. The eolianites vary rapidly in thickness, commonly extending laterally for 10's–100's of meters before pinching-out (Fig. 3E, eolianites 2, 3 and 7). Eolianites 5 and 6 (above paleosol D) are the thickest and most continuous laterally, extending across the entire outcrop. Dune wave-

forms with a 5–15 m amplitude and 20+ m wavelength are preserved in eolianite 3.

Small, but distinct, variations in grain size, composition, degree of cementation, bedding type, dip direction, and lateral continuity are typical of the eolianites. Framework grains are either quartz or carbonate fossil fragments with trace amounts of feldspars and heavy minerals (Fig. 3B). Quartz grains are sub-angular to rounded, monocrystalline or polycrystalline with undulose extinction. Carbonate grains are angular to sub-angular, abraded fragments of bryozoans, bivalves, echinoids, forams and red algae in approximate order of abundance. Carbonate grains and cement comprise 31–56% of the sediment, with the largest percentage in eolianites 5–7 (Fig. 3A). The quartz fraction has a mode in the fine sand size (190–300 μm) and is consistently finer grained than the carbonate grains. Maximum grain size of the carbonate fraction coarsens upward from medium sand (450 μm) in eolianites 1, 3 and 4 to coarse sand ($\sim 1000 \mu\text{m}$) in eolianites 7–9. The eolianites retain substantial porosity. Sparry calcite cement forms a thin rim around framework grains and may show meniscus and pendant fabrics. Degree of cementation varies markedly within individual cross-bed sets and between eolianite units.

Bedding styles range from horizontal and wavy to trough cross-bedded and planar tabular cross-bedded, with all three types occurring in all eolianite units. Planar tabular cross-bed sets dip at angles up to 35°, indicating clearly the eolian origin of the sediments, and commonly exceed 15 m in thickness in eolianites 2, 5 and 7, reaching a maximum of 25 m in eolianite 5 (Fig. 3C). Individual beds within cross-bed sets range from 0.5 to 3 cm thick. Dip direction of planar tabular cross beds is predominantly to the east-northeast in eolianites above paleosol D, and to the east-southeast in eolianites below paleosol D (Fig. 3A), i.e. deposition by predominantly westerly winds.

5.2. Buried paleosols

Buried paleosols can be traced laterally along the cliff face, although they bifurcate and merge to varying extents (Fig. 3E). The most laterally continuous provide key marker beds for stratigraphic correlations. The buried paleosols are Aridosols with either petrocalcic, calcic or cambic B-horizons, and range in thickness from 10 to 90+ cm and in color from yellowish brown (10YR7/6) through pinkish gray (7.5YR7/2). Soil nomenclature follows Soil Survey Staff (1975, 2003) and Munsell soil colors. The paleosols contain less carbonate than the host eolianite (5–25% less in the upper part of the profile) but much more quartz silt (10–30% compared to 0–5%). Calcic B-horizons with stage 1 development (Gile et al., 1981) are most common. The upper parts of all paleosols have disseminated charcoal up to 1 cm in size, pulmonate land snails (*Stylommatophora*), and extensive root bioturbation, with calcified root linings penetrating up to 2 m into the underlying eolianite. Calcified tree trunks 2+ m in diameter

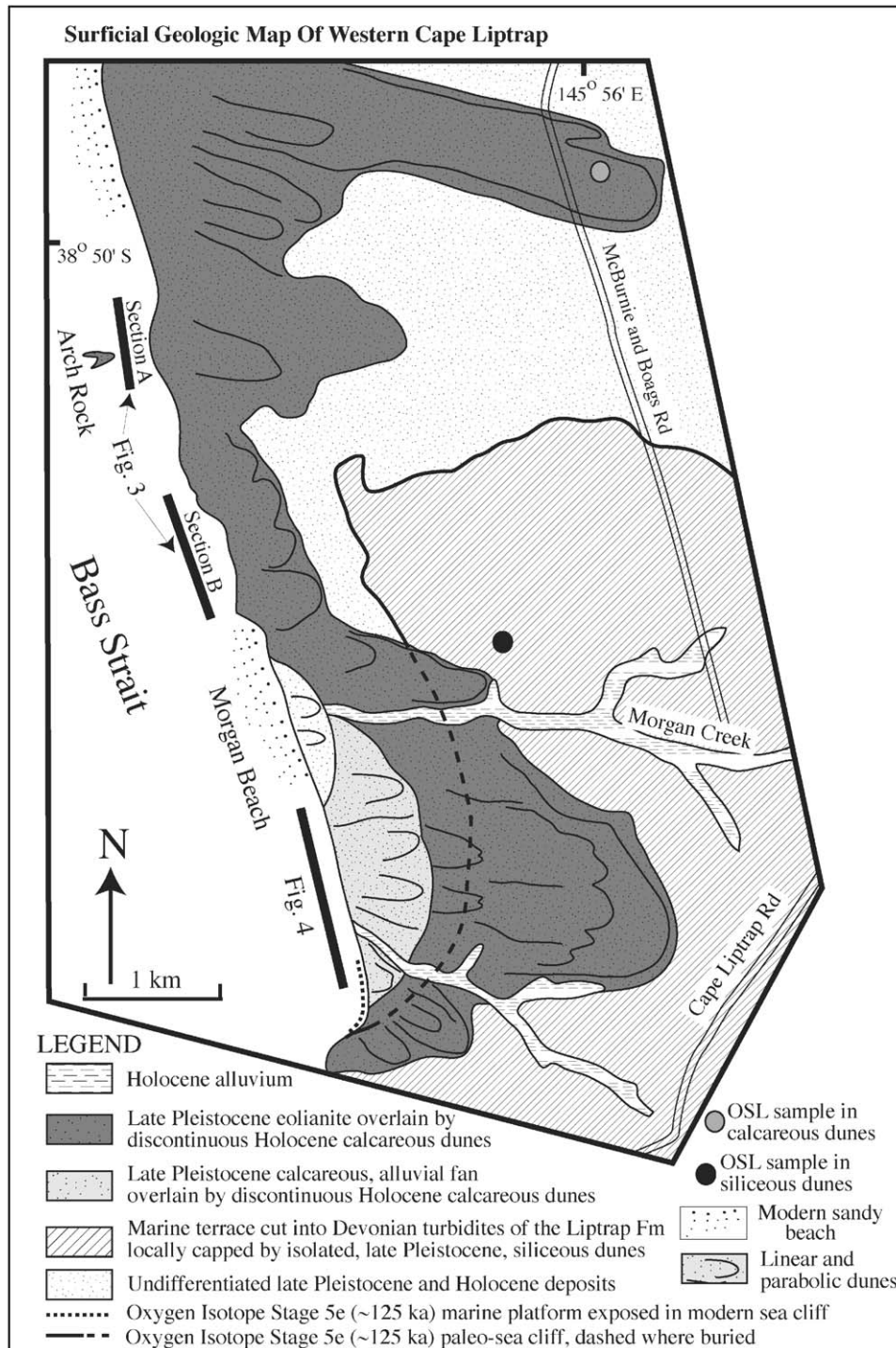


Fig. 2. Surficial geologic map of the western side of Cape Liptrap. Solid bars along coast indicate location of eolianite in the sea cliff sections at Arch Rock (Fig. 3) and the alluvial fan at Morgan Beach (Fig. 4). See Fig. 1C for location. Black dot (siliceous dunes) and grey dot (calcareous dunes) give locations of OSL samples not shown in stratigraphic columns in Figs. 3 and 4. See Fig. 4, column I for age determination of OIS 5 paleo-sea cliff.

may extend upwards into the overlying eolianite. The presence of trees and snails indicate that the paleosols probably had a xeric soil moisture regime, typical of cool, moist winters and warm, dry summers.

Paleosol D is the most well-developed paleosol (Fig. 3D), extending across the entire outcrop (Fig. 3E). It is dark red

(2.5YR4/8), exceeds 90 cm in thickness, and contains 30% quartz silt. The carbonate content in the upper part of the profile is 25% less than the eolianite parent material. It has a petrocalcic horizon with carbonate nodules up to 1 m long extending along bedding planes and a laminar carbonate horizon up to 10 cm thick, locally.

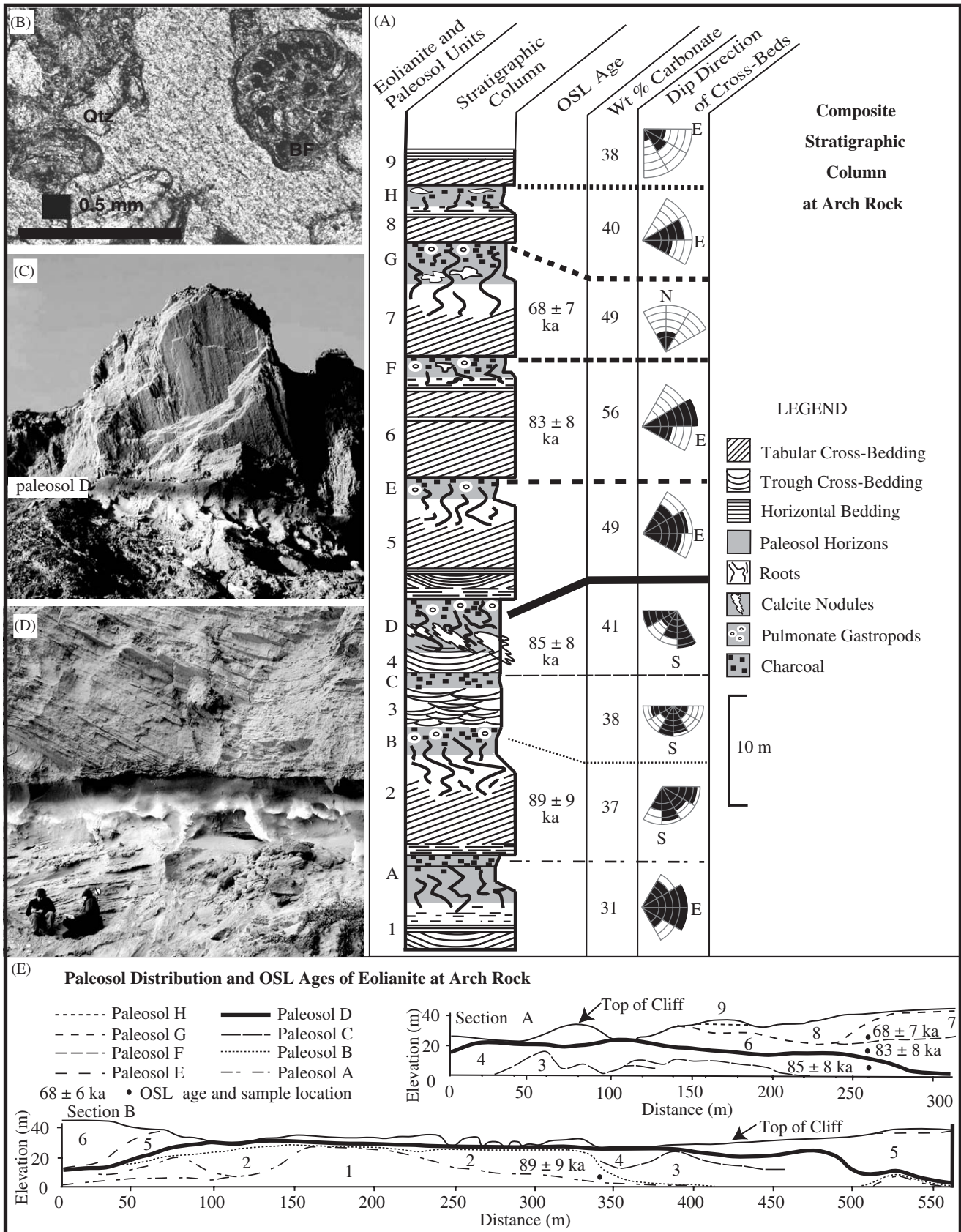


Fig. 3. (A) Composite stratigraphic column of eolianites and paleosols at Arch Rock, OSL ages, weight percent carbonate and cross-bedding dip directions (each concentric circle is 2 observations). (B) Microphotograph of typical eolianite showing sub-rounded quartz (qtz) grains and benthic foram (BF). (C) Dip face of 25m thick, tabular cross-bed sets typical of eolianite 5. Paleosol D is at base of cross-beds. (D) Paleosol D with well-developed petrocalcic horizon (white) and overlying dark red (2.5YR 4/8) B-horizon. OSL sample (85 ± 8 ka) location is to the right of head of person on right. (E) Outcrop distribution of eolianites, buried paleosols, and OSL samples. See Fig. 2 for outcrop location.

5.3. OSL ages

OSL ages decrease systematically from $89 \text{ ka} \pm 9 \text{ ka}$ in eolianite 2 to $68 \text{ ka} \pm 7$ in eolianite 7 (Fig. 3E), indicating a late Pleistocene age for the eolianites in the sea cliffs at Arch Rock (Table 1, TG1–4). All OSL ages are in correct stratigraphic order. However, the age for eolianite 6 ($83 \pm 8 \text{ ka}$) is inconsistent with its position above paleosol D (Fig. 3E, section A at 250 m mark) and the age of the underlying eolianites ($89 \pm 9 \text{ ka}$; $85 \pm 8 \text{ ka}$). Paleosol D is the best developed soil horizon and should represent a substantial period of time; this is consistent with the age of $68 \text{ ka} \pm 7$ for eolianite 7, allowing up to 20 k.y. for development of paleosol D, but conflicts with the age of $83 \pm 8 \text{ ka}$ for eolianite 6. The latter age is therefore regarded as somewhat suspect.

Poorly exposed, calcareous dunes in a small quarry ~3 km inland from the modern Arch Rock sea cliffs along McBurnie and Boags Rd (Fig. 2) yielded an OSL age of $112 \pm 11 \text{ ka}$ (Table 1, AR01), consistent with the geographic location of these dunes landward of the younger eolianites, but seaward of a paleo-sea cliff formed during Oxygen Isotope Stage (OIS) 5e (Fig. 2 near top, discussed further below). Dune orientation (Fig. 2) for these dunes indicates deposition by predominately westerly winds.

6. Morgan beach alluvial fan

6.1. Stratigraphy

Three km south of Arch Rock at Morgan Beach (Fig. 2), Late Pleistocene alluvial fan sediments are exposed along a 1.5 km section of 20+ m high sea cliffs (Fig. 4). Four facies are present: very low angle inclined to horizontally and wavy laminated sands (Fig. 5A), planar tabular cross-bedded sands (Fig. 5B), lenses of angular pebbles and cobbles (Fig. 5C), and finely laminated, horizontally bedded clay (Fig. 5D). Compositionally and texturally, the sandy facies is indistinguishable from the eolianites, consisting of fine quartz sand and medium to coarse sand-sized carbonate fossil fragments (Fig. 5E) in roughly the same proportions as in the eolianites.

The most common facies is low angle inclined to horizontal and wavy laminated sand, which makes up the lower parts of all stratigraphic columns. The facies consists of broad, internally truncated and overlapping lenses, 1–2 m thick and 5–10 m long. A planar tabular cross-bedded unit in the central part of the sequence (Fig. 4, column F) extends up to 80 m laterally. It is composed of 20–200 cm thick cross-bed sets that consistently dip to the south and southeast (Fig. 5F). All stratigraphic columns (except column A) coarsen upward into pebble and cobble lenses containing angular sandstone clasts 1–12 cm in diameter derived from the turbidites of the underlying Devonian Liptrap Formation. The clasts occur either in matrix-free lenses 10–70 cm thick and 10's of meters long, or floating in a matrix of horizontal to wavy bedded sand

or clay. Meter-thick grey-green clay beds with millimeter thick laminae occur near the top of most stratigraphic columns. These finely laminated clays are interbedded with ribbons of black organic material up to 1 cm thick, horizontally to wavy bedded sands and lensoidal pebble layers.

The alluvial fan sequence is overlain by a laterally extensive (Fig. 4, all columns) but poorly developed, organic-rich paleosol up to 1.2 m thick littered with numerous aboriginal occupation sites. The paleosol is overlain by a set of late Holocene dunes and paleosols (Fig. 4, columns F–J).

Underlying the alluvial fan to the northwest is a 1.2 m thick sandy peat (Fig. 4, column A). Elsewhere the alluvial fan sediments overlie massive to horizontally bedded, sub-angular to rounded, organic-rich, grey-green, fine quartz sand interbedded with occasional layers of angular sandstone cobbles and pebbles derived from the Liptrap Formation (Fig. 4, columns I and J). To the southeast the grey-green sand overlies a marine platform cut into the turbidites of the Liptrap Formation (Fig. 4, columns I and J). The sea cliff at the landward edge of this platform, exposed to the south of the Morgan Beach alluvial fan (Fig. 2), was the source of the angular sandstone clasts.

Palynomorph analysis (Partridge, A. D., personal communication, 2003) of the underlying peat (Fig. 4, column A) yielded angiosperm pollen (>75%), with secondary spores (<25%). The palynomorphs are dominated by the Compositae/Asteraceae pollen *Tubulifloridites pleistocenicus* and *T. simplis* which account for 25% of the assemblage, followed by *Myrtaceidites* pollen (16%), *Monotocidites galeatus* (12.5%) and *Banksiaeidites minimus* (10.7%). Pollen of the swamp plants *Haloragacidites haloragoides*, *Milfordia incerta* and *Cyperaceae* pollen are a minor component (9%), as are algal cysts of Zygnemataceae (<1%). The palynomorph assemblage is similar to that reported from Holocene peat profiles on Wilson Promontory (Hope, 1974; Ladd, 1979), and represents the *T. pleistocenicus* Zone (Partridge, 1999) with a broad Late Pliocene to Pleistocene age range.

6.2. Sedimentology

Facies reconstructions (Fig. 4) indicate that the alluvial fan sands accumulated in broad, shallow channels 10's of meters wide and less than a meter deep. Dunes and bars migrated southwards down the deeper channels during flood events, depositing minor tabular and trough cross bedding. However, the dominance of horizontal and wavy bedding indicates that sheet flooding was an important transport process. The alluvial fan sediments coarsen upward because stripping of the eolian cover exposed the sea cliff eroded into fractured Liptrap Formation turbidites (Fig. 2). This provided the fluvial system with an abundant supply of fresh, angular clasts. These clasts were transported short distances onto the fan either as open framework sheet flood deposits or matrix-supported debris

Late Pleistocene Alluvial Fan and Holocene Dunes at Morgan Beach

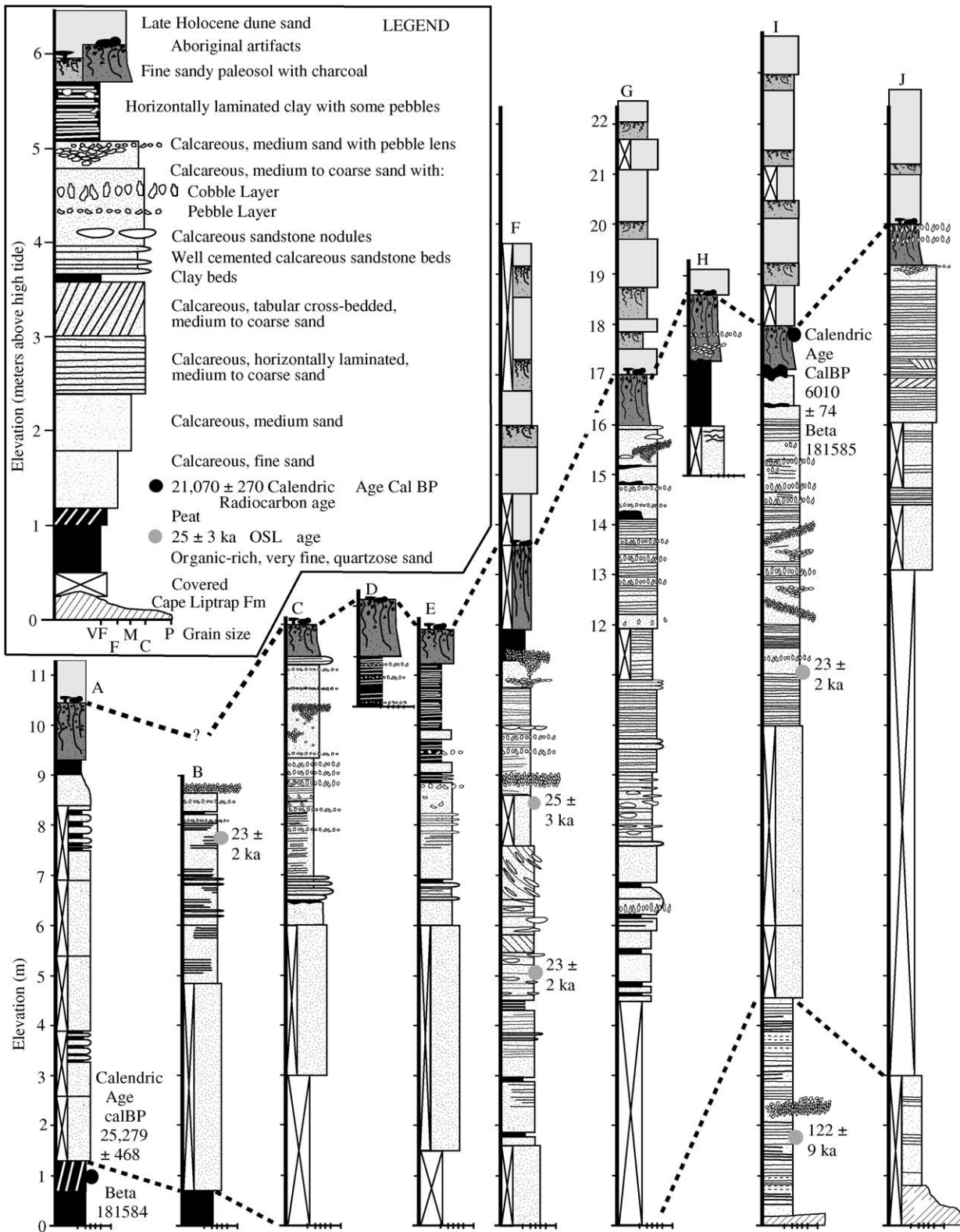


Fig. 4. Stratigraphic columns of the calcareous alluvial fan facies exposed in sea cliffs at Morgan Beach. Horizontal distance between sections A and J is approximately 1.5 km. Note increase in pebbles and clay up-section. Radiocarbon ages are reported as Calendric Age Cal BP using the calibration curve CalPal2004_SFCP and list the Beta Analytic sample number. Legend: VF, very fine sand; F, fine sand; M, medium sand; C, coarse sand; P, pebbles. See Fig. 2 for outcrop location.

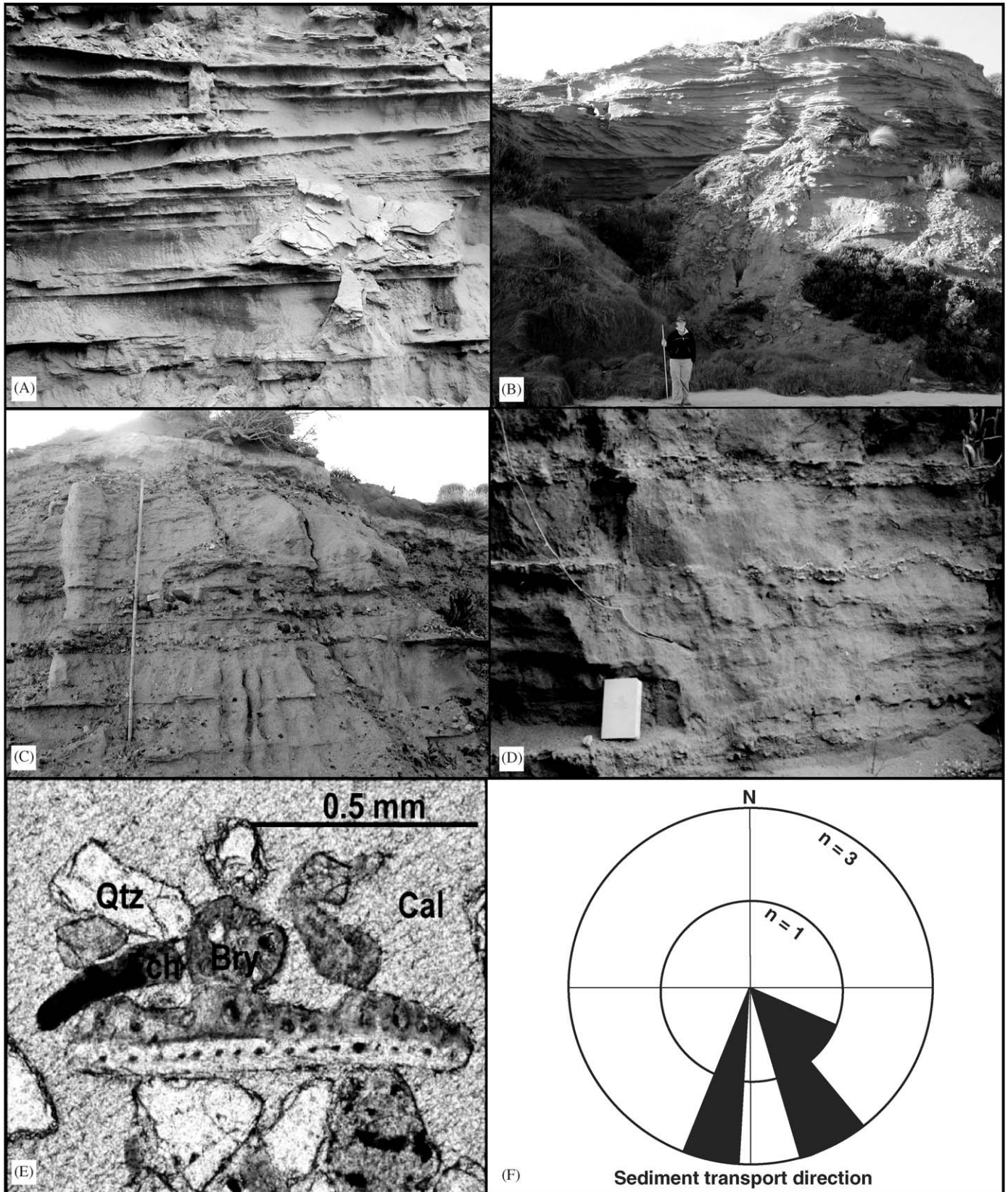


Fig. 5. Photographs of sedimentary facies in alluvial fan. (A) Low angle inclined to horizontally and wavy laminated facies. (B) Planar tabular cross-bedded facies. (C) Lensoidal angular pebble and cobbles beds. (D) Finely laminated clay with pebble layers. (E) Microphotograph of alluvial fan sand showing grain composition: Qtz, quartz; Ech, echinoid; Bry, bryozoan; Cal, sparry calcite cement. (F) Dip direction of planar tabular cross-beds.

flows, indicating ephemeral, but intense runoff conditions within the drainage basin. The interbedded, finely laminated clay beds at the top of the alluvial fan sequence probably represent overbank flood deposits or deposition in small, shallow depressions on the fan surface.

6.3. Radiometric and OSL ages

The alluvial fan yielded four OSL ages ranging from 23 ± 2 ka to 25 ± 3 ka (Table 1, TG5-8 and MB01, Fig. 4), and is bracketed by an overlying paleosol (6010 ± 74 yr cal BP; Fig. 4, column I) and underlying peat ($25,279 \pm 468$ yr cal BP; Fig. 4, column A). These ages indicate very rapid deposition of the alluvial fan during a brief time interval around 23 ka, preceding the Late Glacial Maximum (LGM) at 17–20 ka in southeastern Australia, but within the period of periglacial activity (16–23 ka) in this region (Barrows et al., 2002).

The alluvial fan sediments and basal peat overlie quartz sand (Fig. 4, column I) that yielded an OSL age of 122 ± 9 ka (Table 1, MB01), indicating deposition during the last interglacial sea level highstand (OIS 5e) around 116–128 ka (Muhs, 2002). These sediments rest on a marine platform cut into the turbidites of the Liptrap Formation (Fig. 4, columns I and J). The inner edge of this marine platform outcrops along the south edge of Morgan Beach (Fig. 2) at an elevation of 2.7 m amsl. This elevation is generally consistent with the modeled elevation of the last interglacial sea level maximum (Bintanja et al., 2005) and the elevation of the last interglacial marine terraces along stable parts of the southern Australia coast (Murray-Wallace and Belperio, 1991; Bourman et al., 1999; Murray-Wallace, 2002). Landward of the OIS 5e marine terrace is a paleo-sea cliff that extends northwards parallel to the coast and is partially buried by calcareous dunes. North of Morgan Creek the paleo-sea cliff bends sharply to the east (Fig. 2).

7. Siliceous eolian deposits

7.1. Stratigraphy and sedimentology

Siliceous dunes are locally well developed east of the Cape Liptrap Rd that runs along the highest part of the peninsula (Fig. 6), but are isolated and poorly expressed to the west. They lie on a series of marine terrace ranging in elevation from 35 m to ~160 m and are mostly linear and oriented northwest–southeast (Fig. 6). There are also irregularly shaped coppice dunes, poorly expressed parabolic dunes, and sheet sands. The parabolic dunes show that the wind blew from the northwest, contrasting with the present southwesterly wind direction (Bureau of Meteorology, 2004), which is reflected in the orientation of modern calcareous dunes along the coast (Hill and Bowler, 1995).

Bedding within the siliceous dunes is poorly expressed and they appear massive in outcrop. Compositionally, the

dune sand is >97% sub-angular to well-rounded quartz grains that are monocrystalline or polycrystalline with undulose extinction (Fig. 7C and D). Trace amounts of hornblende, plagioclase, orthoclase, microcline, chalcedony and rock fragments are present. The siliceous dune sands are moderately to well sorted with a modal size of very fine to fine sand (100–150 μ m). Iron oxide staining is present on most grains.

The immediate source of the siliceous eolian sands is the fine sand overlying the marine terraces on the Cape Liptrap peninsula. These sands are thickest on the eastern side of the peninsula where the siliceous dunes are best developed. The marine terrace sands are similar to the modern beach deposits of adjacent Waratah Bay. However, based on shape there are two rather distinct populations of quartz grains: a minor well-rounded fraction and a much more abundant angular to sub-angular fraction (Fig. 7C and D). The sub-angular quartz grains were ultimately derived from the Wilson Promontory Granite, as shown by the trace amounts of non-quartz granitic minerals present. The small component of rounded quartz grains was probably eroded from the sandstone beds of the underlying Liptrap Formation.

7.2. Paleosols and OSL ages

Paleosols on the siliceous sand dunes are actively forming Spodosols up to 1.8 m thick (Fig. 7A and B). They have a well-developed A-horizon (pH 5.1–5.3) overlying a moderately developed, brown (10YR4/30) to brownish yellow (10YR6/8), spodic B-horizon (pH 5.4–5.8). No buried paleosols are present, indicating only a single, brief phase of siliceous dune deposition.

The five OSL ages for the siliceous sand dunes on the eastern side of Cape Liptrap are tightly constrained (19 ± 2 ka to 24 ± 2 ka; Table 1), and match the single OSL age of 19 ± 2 ka from siliceous dunes on the west side (Fig. 2, Table 1, TG16). These data indicate a very brief, but intense, period of eolian activity that coincides with the high latitude solar insolation minimum at ~22 ka (Berger, 1978; Berger and Loutre, 1991) and a peak in dust flux in ODP core from the eastern Tasman Sea (Hesse and Barrows, 2004).

8. Late pleistocene depositional environments, climate and atmospheric circulation

The nature and age of the eolianites, alluvial fan, siliceous dunes, paleosols and peat can be used to develop a model for Late Pleistocene landscape evolution at Cape Liptrap. Changes in solar insolation, atmospheric circulation and climate (precipitation distribution and temperature), eustatic sea level, and physiography of the exposed continental shelf play a critical role in the evolution of these coastal landforms.

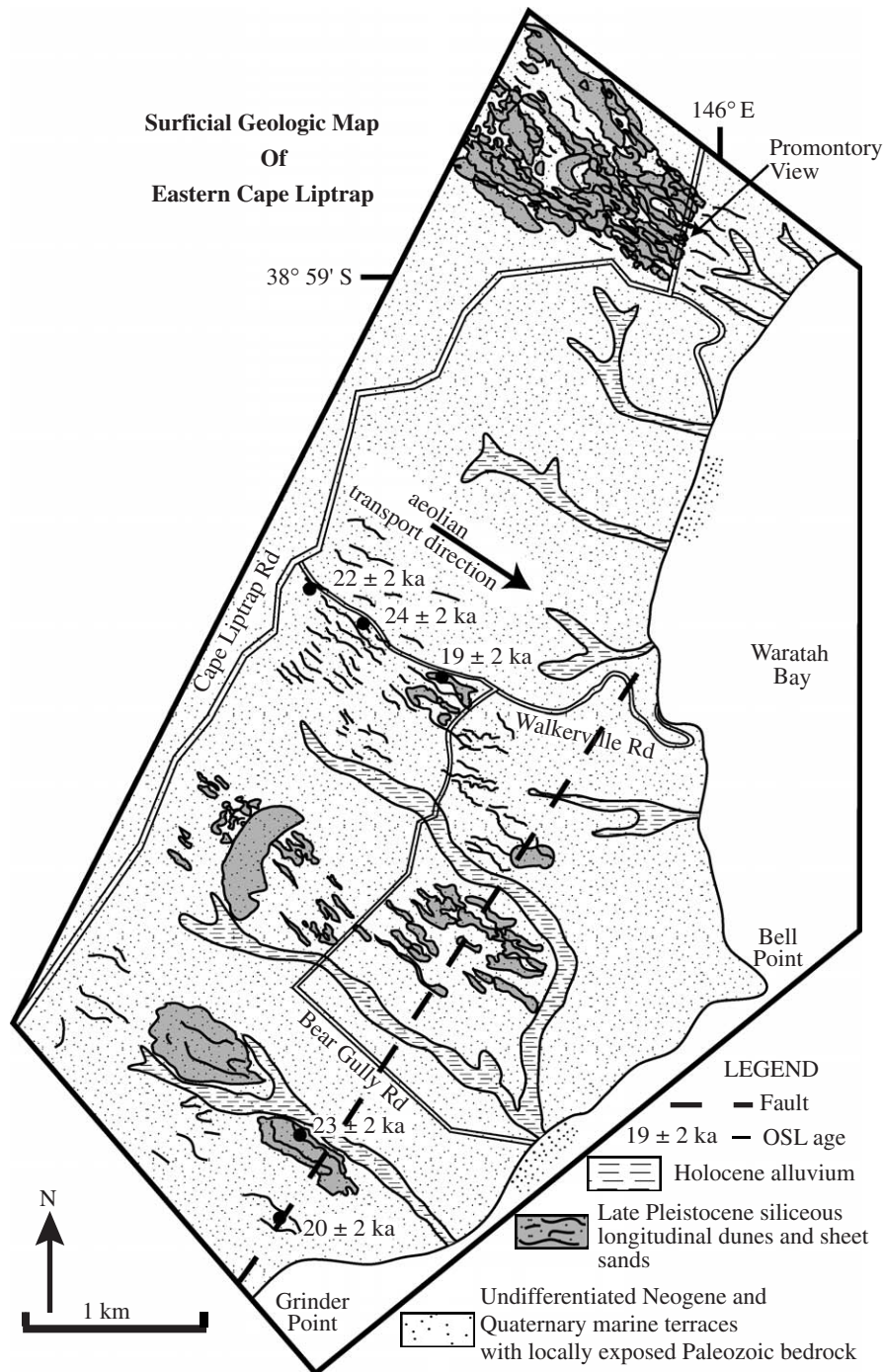


Fig. 6. Surficial geologic map of the central and eastern side of Cape Liptrap. See Fig. 1C for location.

8.1. Interglacial eolianite deposition

The superb sequences of calcareous eolianite dunes in South Australia and western Victoria accumulated during sea level maxima (Boutakoff, 1963; Sprigg, 1979; Jenkin, 1981; Huntley et al., 1993; Murray-Wallace et al., 1999). The youngest eolianite associated with a sea level highstand in the South Australia sequence is the Robe III dune ridge deposited during OIS 5c at ~100 ka (Banerjee et al., 2003).

Eolianites at Arch Rock ~500 km to the east were deposited well after the sea level maximum at ~125 ka (OIS 5e, Fig. 8A), during three main episodes around 115 ± 10 ka (OIS 5e–d transition), $85\text{--}89 \pm 9$ ka (after OIS 5a), and 68 ± 7 ka (OIS 5a–4 transition). Eolianites from the Nepean Peninsula (Spiers, 1992; Zhou et al., 1994) ~150 km west of Cape Liptrap, and from Lord Howe Island (Brooke et al., 2003) ~1400 km northwest of Cape Liptrap in the Tasman Sea, were also deposited during

Siliceous Dune Sands, Eastern Cape Liptrap

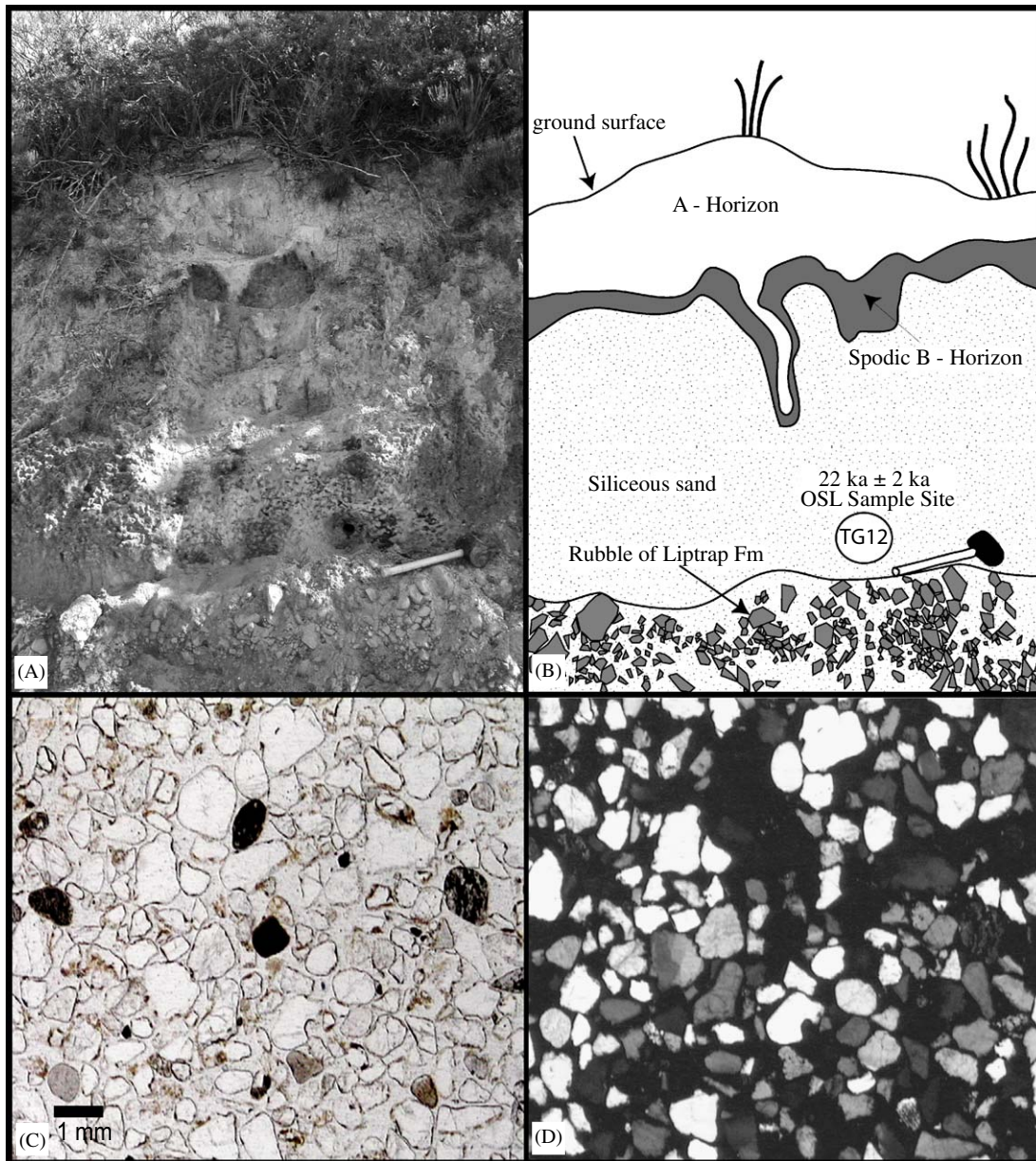


Fig. 7. (A) Section through siliceous dune over Liptrap Formation rubble, showing soil profile and OSL sample location. Intact bedrock occurs at base of photo. Rubber hammer is 30 cm in length. (B) Line drawing of A. (C and D) Microphotograph of siliceous dune sands (C, plane polarized light; D, crossed polars). Note dominance of medium grained, well sorted sub-angular quartz, with smaller amounts of rounded quartz and occasional iron oxide staining.

lower sea levels well after the OIS 5e maximum, based on thermoluminescence (TL) ages of 48–67 ka and 83–94 ka (Neds Beach Formation), respectively.

The eolianites at Arch Rock provide insights into the very sensitive relationship between sea level, sediment supply, sediment mobilization and suitability of depositional space that allows for calcareous eolianite deposition (Brooke et al., 2003). The main calcareous dune construction phases at Arch Rock occurred during periods of rapid sea level fall throughout OIS 5 and into OIS 4 (Fig. 8A). Sea level at the time of deposition of the two youngest Arch Rock eolianites was –35 to –55 m (OIS 5a) and

–60 to –80 m (OIS 4, Fig. 8A), when the shoreline was, respectively 3–5 and 6–12 km seaward of its present position (Fig. 2B, Douglas, 1975). The relatively rapid exposure of the broad shelf (Fig. 2B) provided an abundant source of calcareous shoreface and exposed continental shelf sands. These sands were blown by strong west to west-southwest winds (Figs. 2, 3A and 8B interglacial) onto the abandoned OIS 5e bedrock platform in front of a prominent sea cliff, where all three periods of dune deposition are superimposed. The elevation of this platform at 2+ m amsl preserved the dunes from erosion or submergence during the subsequent sea level rise.

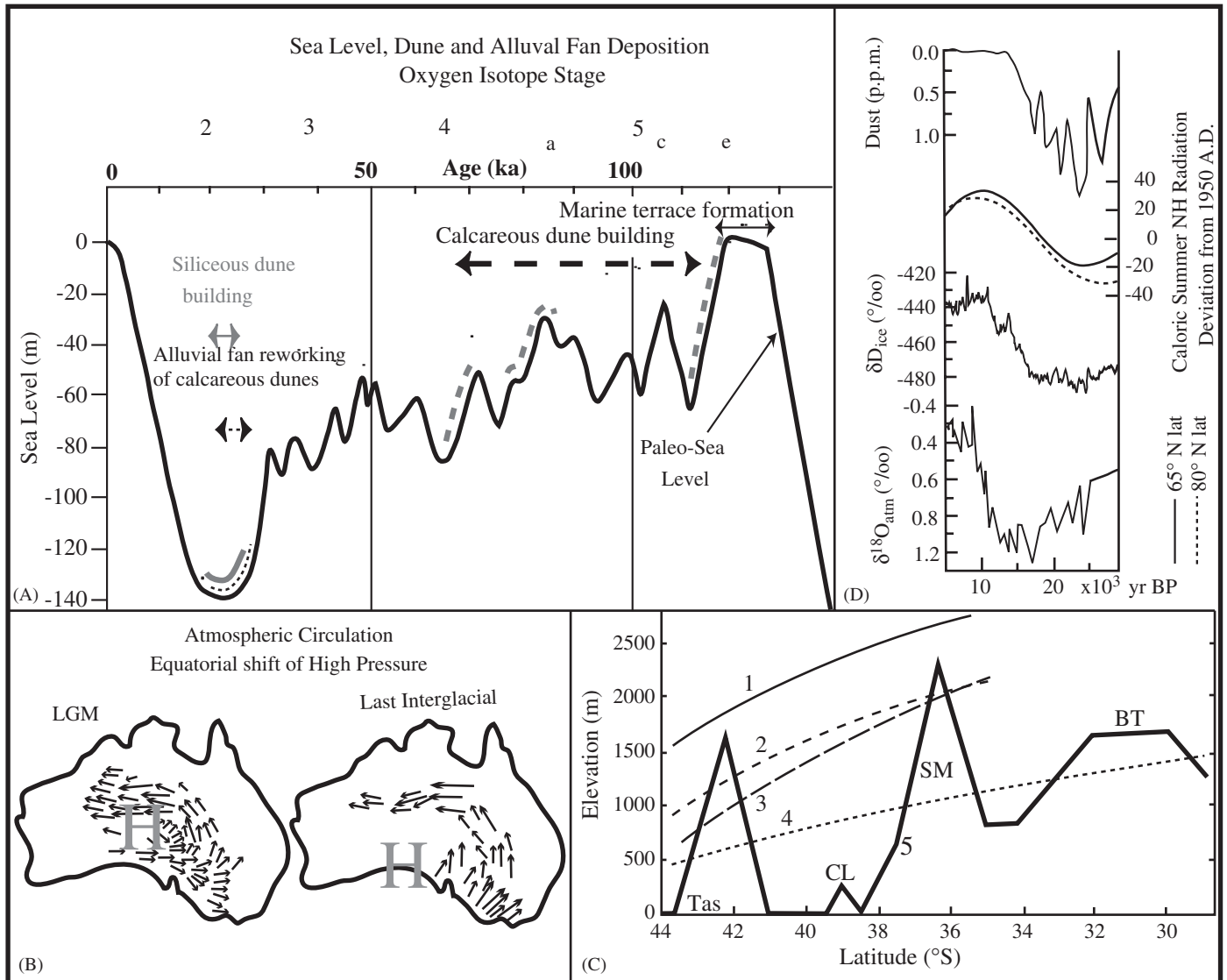


Fig. 8. (A) Timing of eolianite, alluvial fan and siliceous dune deposition relative to eustatic sea level curve (sea level curve from Lambeck and Chappell, 2001); (B) Migration of the southern Australian high pressure cell and change in wind field during glacial/interglacial cycles, modified from Bowler (1976, 1982), Sprigg (1979) and Thom et al. (1994); (C) Modern and LGM snowline and solifluction line for southern Australia and Tasmania; (1) modern snowline; (2) modern limit of solifluction; (3) LGM snowline; (4) LGM lower limit of solifluction; (5) present topography; Tas, Tasmania; CL, Cape Liptrap; SM, Snowy Mountains; BT Barrington Tops; modified from Galloway (1965); (D) high latitude (65°N and 80°N) summer insolation from (Berger, 1978; Berger and Loutre, 1991), $\delta^{18}O_{atm}$, δD_{ice} , and local duct flux from the Vostok ice core (Petit et al., 1999).

Thus, the physiography of the shelf and coastline at Cape Liptrap allowed for the preservation of dune deposition during sea level fall (regression). By contrast, only highstand calcareous dunes were preserved along the South Australian–western Victorian coastline, probably because the dunes that formed there during sea level fall could not be blown far enough inland to avoid submergence during later sea level rises. The shelf in western Victoria–South Australia is more gently sloping, with a gradient of only 0.04° compared to $0.5\text{--}0.7^\circ$ at Cape Liptrap, and the winds are weaker; at present the wind exceeds 30 km/h for only 15% of the year in western Victoria but more than 25% of the year near Cape Liptrap.

8.2. Paleosol formation

Paleosol D, which extends across the entire Arch Rock outcrop (Fig. 3E), divides the eolianites into an upper unit (~ 70 ka) with 5 eolianites and 4 minor paleosols, and a lower unit ($\sim 85\text{--}89$ ka) with 4 eolianites and 3 minor paleosols (Fig. 3A). Paleosol D indicates an extended period (on the order of 10^4 years) of dune stability and soil formation between the intermediate sea level highstands at OIS 4 and OIS 5a. The other seven paleosols are less well developed and frequently bifurcate and merge. Local processes such as fire, tree throw or individual storm events probably destabilized portions of the dune field on much shorter timescales ($10^2\text{--}10^3$ years) resulting in locally

less well developed soils. The presence of abundant charcoal fragments in all paleosols suggests that fire played an important role in dune destabilization during the late Pleistocene. At present human disturbance of vegetation along the coastal cliffs results in dune blowouts that rapidly expand over a few years.

Vegetation cover on the eolianite dunes played a major role in dune stabilization and soil formation. The extensive, deep roots and land snails in all the paleosols and the large preserved tree trunks in some horizons indicate a xeric soil moisture regime and a substantial forest cover. In particular, the well-developed petrocalcic laminar and nodular horizon within paleosol D suggests extended periods of soil moisture evaporation. The high content of wind-blown quartz silt (up to 30%) indicates continued atmospheric dust fallout onto the dune surface during soil formation. The vegetation cover probably limited the local sediment supply, and the eolian silt may have been derived from inland regions, given the voluminous amounts of wind-blown dust deposition over extensive areas of central Australia during dry phases in the Pleistocene (Hesse and McTainsh 2003).

8.3. Alluvial fan deposition at the LGM

Deposition of the alluvial fan during a brief interval around 23 ka preceded the LGM. Erosion of eolianite dunes covering the bedrock sea cliff and the marine terrace landward of Morgan Beach (Fig. 2) supplied abundant sediment to the nearby creeks, exceeding their transport capacity, and rapidly depositing the fan on the abandoned OIS 5e marine platform (Figs. 2 and 4, columns I and J). Reworking of eolianites into alluvial fans has not been previously reported from coastal southeastern Australia, and reflects the particular physiographic conditions present inland of Morgan Beach.

The coarser grained alluvial fan deposits imply locally intense runoff sufficient to transport cobbles several kilometers, probably generated by brief, but intense, storms. These high-energy flood events suggest a change in precipitation intensity around 23 ka. There is evidence of a substantial reduction in rainfall variability and evaporation around the LGM elsewhere in Australia, e.g. increased fluvial activity in the Murrumbidgee river paleochannels (35–13 ka; Page et al., 1996), increased flooding in monsoonal northern Australia 30–18 ka (Nott and Price, 1999), high lake levels for Lake George, NSW (27–21 ka, Coventry and Walker, 1977) and Lake Urana, NSW (30–12 ka, Page et al., 1994), and deposition of fluvial wetlands in the Flinders Ranges (33–17 ka, Williams et al., 2001).

In addition, the increased runoff prior to the LGM at Cape Liptrap may have been driven by low rates of infiltration within the drainage basin, due to increased bedrock exposure and reduced vegetation density during the overall drier and windier climate of the LGM (discussed further below). Nevertheless, the peat under-

lying the alluvial fan, which was deposited in a swamp on the impermeable bedrock terrace, indicates there was sufficient infiltration to maintain local groundwater wetlands.

8.4. LGM climate and landscape response

Previous research has demonstrated major changes in large-scale atmospheric circulation patterns between glacial and interglacial climates in southern Australia (Sprigg, 1979; Bowler, 1976, 1982, 1990; Hill and Bowler, 1995). The southern Australian winter high pressure system migrated northwards during the LGM (Fig. 8B), producing a more continental climate with increased aridity (Bowler, 1976, 1982, 1990; Hill and Bowler, 1995; Nanson et al., 1992; Thom et al., 1994; Johnson et al., 1999; Magee et al., 2004) and temperatures 5–10 °C cooler (Galloway, 1965; Bowden, 1983; Miller et al., 1997; Barrows et al., 2004). The elevation of the equilibrium line decreased (Barrows et al., 2002), so that mountain glaciation and periglacial block fields descended to a minimum elevation of 600 m in southern Australia (Fig. 8C; Galloway, 1965; Barrows et al., 2004). The response of Australian landscapes and ecosystems to the LGM climate changes was complex and varied (Williams, 1994; Bowler, 1986, 2000; Williams et al., 2001). The alluvial fan and siliceous dunes at Cape Liptrap, deposited within a very restricted time span around 23 ka, indicate that eolian transport, periodic extreme storm runoff and mechanical weathering dominated the landscape. This provides insight into the evolution of coastal southeast Australian landscapes in response to global climate forcing and local climatic conditions immediately preceding the LGM.

At Cape Liptrap, the pulse of siliceous dune building and erosion of the calcareous eolianites to form the alluvial fan were probably caused by reduced vegetation cover around 23 ka. Increased wind strength is unlikely to have been responsible for eolian activity, because Bowden (1983) calculated a wind speed of 36 km/h for development of LGM siliceous dunes on the north Tasmanian coast, similar to the average 3PM wind speed at Cape Liptrap today (32 km/h).

The decrease in vegetation cover was due to the drier conditions at Cape Liptrap immediately preceding the LGM. Presently, the ocean nearly surrounds Cape Liptrap, but immediately preceding the LGM sea level was ~125 m lower (Fig. 8A) and the coastline lay ~250 km seaward (Bowden, 1983; Bowler, 1990; Fig. 1B). The strong landward gradient in climatic continentality was probably responsible for increased eolian activity recorded along the southeastern Australian coast at the LGM, e.g. in New South Wales (Nott and Price, 1991; Nanson et al., 1992; Nanson et al., 2003). However, the wider continental shelf would have produced a larger decrease in temperature and rainfall at Cape Liptrap than anywhere else in the region. The mean annual temperature there today is ~14 °C, and it could have been 10 °C colder during the LGM (Miller

et al., 1997; Bintanja et al., 2005). The increasingly continental climate raised the rates of bedrock mechanical weathering, fracturing exposed bedrock (Fig. 7A and B) and supplying angular cobbles to the alluvial fan at Morgan Beach (Fig. 4).

The siliceous dunes that extend across almost the entire Cape Liptrap peninsula form part of an extensive dune field extending northwest of Cape Liptrap, characterized by low dunes with a west-northwest to west orientation (Hill and Bowler, 1995; Joyce et al., 2003) deposited by northwesterly winds (Fig. 6). This contrasts with the present southwesterly wind direction (Bureau of Meteorology, 2004), which is reflected in the modern calcareous dunes along the coast (Hill and Bowler, 1995). The difference in the wind regime was due to the northwards migration of the winter high pressure system during the LGM (Fig. 8B). At present the western side of Cape Liptrap has active calcareous coastal dunes, but calcareous dune activity was absent at the LGM, probably because the source of the carbonate sand (reworked skeletal fragments from the shallow marine environment) lay over 250 km away.

The very restricted age range around 23 ka for the deposits at Cape Liptrap demonstrates a very brief, but significant period of landscape instability due to erosion by both wind and running water. The timing of the coldest, most arid climate at Cape Liptrap accords extremely well with the calculated minimum in high latitude (65° N) summer insolation at ~ 22 ka (Berger, 1978; Berger and Loutre, 1991), the minimum in the deuterium content of Antarctic ice at ~ 22 – 23 ka (a proxy for local air temperature; Petit et al. 1999) and the maximum in dust flux from the Vostok ice core and in ODP cores in the eastern Tasman Sea at 21 – 23 ka (Petit et al. 1999; Hesse and Barrows, 2004). However, the maximum landscape instability phase at Cape Liptrap precedes by several thousand years the minimum in sea surface temperatures at 20.5 ± 1.5 ka in the Southern Ocean and Tasman Sea (Barrows et al., 2000; Barrows and Juggins, 2005), the maximum reported glacial advances in the Southeast Australia highlands at ~ 17 to ~ 20 ka (Barrows et al., 2001; Barrows et al., 2002) and the minimum ^{18}O content of trapped air (a proxy for global ice volume) from the Vostok ice core at ~ 17 ka (Petit et al., 1999). This reflects the fact that there is a time lag of perhaps 3 ka between the insolation minimum and the maximum glacial advance. This indicates that those climate parameters which respond quickly to a decrease in solar insolation (e.g. air temperature, rainfall effectiveness) show an earlier minimum than parameters linked to the ice volume (e.g. sea surface temperatures). Thus, those landscape and ecosystem properties that respond quickly to changes in air temperature, windiness, and rainfall effectiveness (e.g. vegetation type, distribution and density, mechanical weathering, runoff effectiveness, and eolian and fluvial activity) should coincide with climatic forcing from changes in solar insolation. The Cape Liptrap data

demonstrate that the most unstable landscape phase, with the coldest, most arid climate preceded the LGM by several thousand years in southeastern Australia and was short-lived, probably only ~ 3 ka, given the very restricted age range for dune mobility and alluvial fan deposition.

9. Conclusions

The three main phases of calcareous eolianite deposition at Arch Rock coincide with sea level fall after OIS 5e (~ 115 ka) and 5a (85–89 ka) and during OIS 4 (~ 70 ka). This indicates that the rapid exposure of coastal nearshore platforms is a necessary condition for development of a sufficient source of calcareous sand. This also implies that regressive phases of sea level tend to allow for better preservation of calcareous eolianite. Variable west-southwesterly winds blew sand 5–12 km onshore at Arch Rock from the active shoreface on the exposed continental shelf to form 9 eolianite units separated by paleosols. The paleosols contain abundant quartz silt, extensive calcified root systems, charcoal and land snails, indicating that a well-developed vegetation cover stabilized the dunes and trapped atmospheric dust fallout. Local conditions such as fire caused short-term dune instability on the time scale of 10^2 – 10^3 years.

Alluvial fan, peat and siliceous dune deposition at Cape Liptrap occurs during a very restricted period around 23 ka. This phase of maximum landscape instability coincides well with solar insolation and air temperature minimum and dust flux maximum. It precedes by several thousand years the minimum in sea surface temperature, global ice volume maximum and most extensive glaciation in the southeast Australian highlands. The climate immediately preceding the LGM was more continental (colder and drier) than at present with less vegetation cover, intensified mechanical weathering, and ephemeral, but intense, surface runoff from a change in precipitation intensity and distribution. The predominant wind direction was northwesterly, contrasting with the present southwesterly orientation, due to the northwards migration of the winter high-pressure system.

Acknowledgments

We thank J. Bowler, M. Orr, M. Sandiford, and A. Vandenberg for stimulating discussions in the field, Heather and David Bligh of the Toora Tourist Park for logistical support, and Tony and Elizabeth Landy and the Jelbert family for critical land access. Gresley Wakelin-King and John Olley provided known dose recovery data of OSL samples. M. Cupper provided ages for OSL samples AR01 and MB01. G. Nanson, V. Gostin and M. Cupper provided critical reviews of an earlier draft of the manuscript.

References

- Adamiec, G., Aitken, M.J., 1998. Dose-rate conversion factors: update. *Ancient TL* 16, 37–50.
- Baker, G., 1956. Sand drift at Portland, Victoria. *Proceedings of the Royal Society of Victoria* 68, 151–197.
- Banerjee, D., Hildebrand, A.N., Murray-Wallace, C.V., Bourman, R.P., Brooke, B.P., Blair, M., 2003. New quartz SAR-OSL ages from the stranded beach dune sequence in south-east South Australia. *Quaternary Science Reviews* 22, 1019–1025.
- Barrows, T.T., Juggins, S., 2005. Sea-surface temperatures around the Australian margin and Indian Ocean during the Last Glacial Maximum. *Quaternary Science Reviews* 24, 1017–1047.
- Barrows, T.T., Juggins, S., De Deckker, P., Thiede, J., Martinez, J.I., 2000. Sea-surface temperatures of the southwest Pacific Ocean during the Last Glacial Maximum. *Paleoceanography* 15, 95–109.
- Barrows, T.T., Stone, J.O., Fifield, K.L., Cresswell, R.G., 2001. Late Pleistocene glaciation of the Kosciuszko massif, Snowy Mountains, Australia. *Quaternary Research* 55, 179–189.
- Barrows, T.T., Stone, J.O., Fifield, L.K., Cresswell, R.G., 2002. The timing of the last glacial maximum in Australia. *Quaternary Science Reviews* 21, 159–173.
- Barrows, T.T., Stone, J.O., Fifield, L.K., 2004. Exposure ages for Pleistocene periglacial deposits in Australia. *Quaternary Science Reviews* 23, 697–708.
- Berger, A., 1978. Long-term variations of caloric insolation resulting from the earth's orbital elements. *Quaternary Research* 9, 139–167.
- Berger, A., Loutre, M.F., 1991. Insolation values for the climate of the last 10 million years. *Quaternary Science Reviews* 10, 297–317.
- Bintanja, R., van de Wal, R., Oerlemans, J., 2005. Modelled atmospheric temperatures and global sea levels over the past million years. *Nature* 437, 125–128.
- Bird, E.C.F., 1961. The coastal barriers of east Gippsland, Australia. *Journal of Geography* 127, 460–468.
- Blackburn, G., 1962. Stranded coastal dunes in northwestern Victoria. *Australian Journal of Science* 9, 388–389.
- Bøtter-Jensen, L., Duller, G.A.T., 1992. A new system for measuring OSL from quartz samples. *Nuclear Tracks and Radiation Measurements* 20, 549–553.
- Bøtter-Jensen, L., Bulur, E., Duller, G.A.T., Murray, A.S., 2000. Advances in luminescence instrument systems. *Radiation Measurements* 32, 523–528.
- Bourman, R.P., Belperio, A.P., Murray-Wallace, C.V., Cann, J.H., 1999. A last glacial embayment fill at Normanville, South Australia, and its neotectonic implications. *Transactions of the Royal Society of South Australia* 123, 1–15.
- Boutakoff, N., 1963. The geology and geomorphology of the Portland area. *Geological Society of Victoria, Memoir* 22.
- Bowden, A., 1983. Relict terrestrial dunes: legacies of a former climate in coastal northeastern Tasmania. *Zeitschrift für Geomorphologie N.F. Supplementband* 45, 153–174.
- Bowler, J.M., 1976. Aridity in Australia: age, origins and expression in aeolian landforms and sediments. *Earth Science Reviews* 12, 279–310.
- Bowler, J.M., 1982. Aridity in the late Tertiary and Quaternary of Australia, Paper 4. In: Barker, W.R., Greenslade, P.J.M. (Eds.), *Evolution of Flora and Fauna of Arid Australia*. Peacock Publications, South Australia, pp. 35–45.
- Bowler, J.M., 1986. Spatial variability and hydrologic evolution of Australian lake basins: analogue for Pleistocene hydrologic change and evaporite formations. *Paleogeography, Paleoclimatology, Paleocology* 54, 21–41.
- Bowler, J.M., 1990. From Sand Dunes to Tall Timber: Environmental Impact in South Gippsland. South Gippsland Conservation Society, Press Gallery, Leongatha.
- Bowler, J.M., 2000. Pluvial aspects of the LGM. Abstracts, Department of Geology, Australian National University, Quaternary Studies Meeting, Canberra, 7–9 February 2000, pp. 11–12.
- Brooke, B.P., Murray-Wallace, C.V., Woodroffe, C.D., Hejnis, H., 2003. Quaternary aminostratigraphy of eolianite on Lord Howe Island, southwest Pacific Ocean. *Quaternary Science Reviews* 22, 387–406.
- Bureau of Meteorology, 2004. Climate Averages and Extremes <http://www.bom.gov.au/climate>.
- Cook, P.J., Colwell, J.B., Firman, J.M., Lindsay, D.A., Schwebel, D.A., Von der Borch, C.C., 1977. The Late Cainozoic sequence of southeast South Australia and Pleistocene sea level changes. *Journal of Australian Geology and Geophysics* 2, 81–88.
- Coventry, R.J., Walker, P.H., 1977. Geomorphical significance of late Quaternary deposits of the Lake George area, NSW. *Australian Geographer* 13, 369–376.
- Douglas, J.G., 1975. Liptrap and Part of the Yanakie. Geological Survey of Victoria, Parts 8020 and 8120, Zone 55, Map Scale 1:63,360, Melbourne.
- Duller, G.A.T., 1999. Analyst Version 2.12. Luminescence Laboratory, University of Wales, Aberystwyth, UK.
- Galbraith, R.F., Roberts, R.G., Laslett, G.M., Yoshida, H., Olley, J.M., 1999. Optical dating of single and multiple grains of quartz from Jinnium Rock Shelter, northern Australia. Part I: experimental design and statistical models. *Archaeometry* 41, 339–364.
- Galloway, R.W., 1965. Late Quaternary climates in Australia. *Journal of Geology* 73, 603–617.
- Gile, L.H., Hawley, J.W., Grossman, R.B., 1981. Soils and Geomorphology in the Basin and Range area of southern New Mexico—Guidebook to the Desert Project. New Mexico Bureau of Mines and Mineral Resources Memoir 39.
- Hesse, P., Barrows, T., 2004. Silk Purse≠sow's Ear: Difficulties in Obtaining a High Resolution Record of Dust Flux from Sedimentation Rate Deep-sea Sediments. OZ—Intimate Workshop, Australian National University, Canberra.
- Hesse, P.P., McTainsh, G.H., 2003. Australian dust deposits: modern processes and the Quaternary record. *Quaternary Science Reviews* 22, 2007–2035.
- Hill, S.M., Bowler, J.M., 1995. Linear dunes at Wilson's Promontory and South-East Gippsland, Victoria: relict landforms from periods of past aridity. *Proceedings of the Royal Society of Victoria* 107, 73–81.
- Hope, G.S., 1974. The vegetation history from 6000 BP to present of Wilson's Promontory, Victoria. *New Phytologist* 73, 1035–1053.
- Huntley, D.J., Hutton, J.T., Prescott, J.R., 1993. The stranded beach-dune sequence of south-east South Australia: a test of thermoluminescence dating, 0–800 ka. *Quaternary Science Reviews* 12, 1–20.
- Jenkin, J.J., 1968. The geomorphology and upper caenozoic geology of south-east Gippsland, Victoria. *Geological Society of Victoria, Memoir* 27.
- Jenkin, J.J., 1981. Evolution of the Victorian coastline. *Proceedings of the Royal Society of Victoria* 99, 37–54.
- Jenkin, J.J., 1988. Geomorphology, Chapter 10. In: Douglas, J.G., Ferguson, J.A. (Eds.), *Geology of Victoria*. Victoria Division, Geological Society of Australia, Melbourne, pp. 403–426.
- Jenkin, J.J., Lawrence, C.R., Kenley, P.R., Gill, E.D., Macumber, P.G., Neilson, J.L., 1988. Quaternary, Chapter 9. In: Douglas, J.G., Ferguson, J.A. (Eds.), *Geology of Victoria*. Victoria Division, Geological Society of Australia, Melbourne, pp. 351–402.
- Johnson, B.J., Miller, G.H., Fogel, M.L., Magee, J.W., Gagan, M.K., Chivas, A.R., 1999. 65,000 years of vegetation change in central Australia and the Australian summer monsoon. *Science* 284, 1150–1153.
- Joyce, E.B., Webb, J.A. (co-ordinators), Dahlhaus, P.G., Grimes, K.G., Hill, S.M., Kotsonis, A., Martin, J., Mitchell, M.M., Neilson, J.L., Orr, M.L., Peterson, J.A., Rosengren, N.J., Rowan, J.N., Rowe, R.K., Sargeant, I., Stone, T., Smith, B.L., White, S., 2003. Chapter 18—Geomorphology. In: Birch, W. (Ed.), *Geology of Victoria*, vol. 23. Geological Society of Australia Special Publication, pp. 533–561.
- Kenley, P.R., 1971. Cainozoic geology of the eastern part of the Gambier Embayment, south-western Victoria. In: Wopfner, H., Douglas, J.G. (Eds.), *The Otway Basin of south-eastern Australia*. Special Publication, Geological Surveys of South Australia and Victoria, pp. 89–153.

- Kenley, P.R., 1976. Southwestern Victoria. Geological Society of Australia Special Publication No. 5, pp. 290–298.
- King, D., 1960. The sand ridge deserts of South Australia and related aeolian landforms of the arid cycles. *Transactions of the Royal Society of South Australia* 89, 99–160.
- Ladd, P.G., 1979. A Holocene vegetation record from the eastern side of Wilsons Promontory, Victoria. *New Phytologist* 82, 265–276.
- Lambeck, K., Chappell, J., 2001. Sea level change through the last glacial cycle. *Science* 292, 679–686.
- Magee, J.W., Miller, G.H., Spooner, N.A., Questiaux, D., 2004. Continuous 150 k.y. monsoon record from Lake Eyre, Australia: Insolation-forcing implications and unexpected Holocene failure. *Geology* 32, 885–888.
- Miller, G.H., Magee, J.W., Jull, A.J.T., 1997. Low-latitude glacial cooling in the Southern Hemisphere from amino-acid racemization in emu eggshells. *Nature* 385, 241–244.
- Muhs, D., 2002. Evidence for the timing and duration of the last interglacial period from high-precision uranium-series ages of corals on tectonically stable coastlines. *Quaternary Research* 58, 36–40.
- Murray, A.S., Wintle, A.G., 2000. Luminescence dating of quartz using an improved single-aliquot regenerative-dose protocol. *Radiation Measurements* 32, 57–73.
- Murray-Wallace, C.V., 2002. Pleistocene coastal stratigraphy, sea level highstands and neotectonism of the southern Australia continental margin—a review. *Journal of Quaternary Science* 17, 469–489.
- Murray-Wallace, C.V., Belperio, A.P., 1991. The last interglacial shoreline in Australia—a review. *Quaternary Science Reviews* 10, 441–461.
- Murray-Wallace, C.V., Belperio, A.P., Bourman, R.P., Cann, J.H., Price, D.M., 1999. Facies architecture of a last interglacial barrier: a model for Quaternary barrier development from the Coorong to Mount Gambier Coastal Plain, southeastern Australia. *Marine Geology* 158, 177–195.
- Murray-Wallace, C.V., Brooke, B.P., Cann, J.H., Belperio, A.P., Bourman, R.P., 2001. Whole-rock aminostratigraphy of the Coorong Coastal Plain, South Australia: towards a 1 million year record of sea-level highstands. *Journal of the Geological Society of London* 158, 111–124.
- Nanson, G.C., Price, D.M., Short, S.A., 1992. Wetting and drying of Australia over the past 300 ka. *Geology* 20, 791–794.
- Nanson, G.C., Cohen, T.J., Doyle, J., Price, D.M., 2003. Alluvial evidence of late-Quaternary climate and flow-regime changes on the coastal rivers of New South Wales, Australia. In: Gregory, K.J., Benito, G. (Eds.), *Palaeohydrology: Understanding Global Change*. Wiley, Chichester, pp. 233–258.
- Nott, J.F., Price, D.M., 1991. Late Pleistocene to early Holocene aeolian activity in the upper and middle Shoalhaven catchment, New South Wales. *Australian Geographer* 22, 168–177.
- Nott, J.F., Price, D.M., 1999. Waterfalls, floods and climate change: evidence from tropical Australia. *Earth and Planetary Science Letters* 171, 267–276.
- Olley, J.M., Murray, A.S., Roberts, R.G., 1996. The effects of disequilibria in the uranium and thorium decay chains on burial dose rates in fluvial sediments. *Quaternary Geochronology* 15, 751–760.
- Oyston, B., 1996. Thermoluminescence dating of quartz from Quaternary aeolian sediments in southeastern Australia. Ph.D. Dissertation, Latrobe University, Bundoora, Victoria.
- Page, K.J., Dare-Edwards, A., Nanson, G., Price, D., 1994. Late Quaternary evolution of Lake Urana, New South Wales, Australia. *Journal of Quaternary Science* 9, 47–57.
- Page, K.J., Nanson, G.C., Price, D., 1996. Chronology of Murrumbidgee river paleochannels on the Riverine plain, Southeastern Australia. *Journal of Quaternary Science* 11, 311–326.
- Partridge, A.D., 1999. Late Cretaceous to Tertiary Geological Evolution of the Gippsland Basin, Victoria, Ph.D. dissertation, La Trobe University, Bundoora, Victoria.
- Petit, J.R., Jonzel, J., Raynaud, D., Barkov, N.I., Barnola, J.-M., Basile, I., Benders, M., Chappellaz, J., Davis, M., Delaygua, G., Delmotte, M., Kotlyakov, V.M., Legrad, M., Lipenkov, V.Y., Lorius, C., Pepin, L., Ritz, C., Salzman, E., Stievenard, M., 1999. Climate and atmospheric history of the past 420,000 years from the Vostok ice core, Antarctica. *Nature* 399, 429–436.
- Prescott, J.R., Hutton, J.T., 1994. Cosmic ray contributions to dose rates for luminescence and ESR dating: large depths and long term variations. *Radiation Measurements* 23, 497–500.
- Price, D.M., Brooke, B.P., Woodroffe, C.D., 2001. Thermoluminescence dating of aeolianites from Lord Howe Island and south-west Western Australia. *Quaternary Science Reviews* 20, 841–846.
- Roberts, R.G., Galbraith, R.F., Olley, J.M., Yoshida, H., Laslett, G.M., 1999. Optical dating of single and multiple grains of quartz from Jimnium Rock Shelter, northern Australia. Part II: Results and implications. *Archaeometry* 41, 365–395.
- Sandiford, M., 2003. Neotectonics of southeastern Australia: linking the Quaternary faulting record with seismicity and in situ stress. In: Hills, R.R., Muller, D. (Eds.), *Evolution and Dynamics of the Australian Plate*, Geological Society of Australia Special Publication No. 22, pp. 101–133.
- Sigle, W.R., Colhoun, E.A., 1982. Terrestrial dunes, man and the late Quaternary environment in south Tasmania. *Paleogeography, Paleoclimatology, Paleocology* 39, 87–121.
- Soil Survey Staff, 1975. *Soil Taxonomy*. Handbook No. 436, second ed. US Department of Agriculture.
- Soil Survey Staff, 2003. *Keys to Soil Taxonomy*, ninth ed. US Department of Agriculture.
- Spiers, R.H., 1992. The geological evolution of Quaternary coastal dune sequences in the Sorrento–Portsea area of the Nepean Peninsula, Victoria, Australia. B.Sc. Thesis (Honours), Latrobe University, Bundoora, Victoria.
- Strigg, R.C., 1979. Stranded and submerged sea-beach systems of southeast South Australia and the aeolian desert cycle. *Sedimentary Geology* 22, 53–96.
- Thom, B., Hesp, P., Bryant, E., 1994. Last glacial “coastal” dunes in eastern Australia and implications for landscape stability during the Last Glacial Maximum. *Paleogeography, Paleoclimatology, Paleocology* 111, 229–248.
- VandenBerg, A.H.M. (compiler), 1997. Warragul, SJ 55-10, second ed., Geological Map Series, Department of Natural Resources and Environment, Victoria, Scale 1:250,000.
- Williams, M., 1994. Some Implications of past climate change in Australia. *Transactions of the Royal Society of South Australia* 118, 17–25.
- Williams, M., Prescott, J.R., Chappell, J., Adamson, D., Cock, B., Walker, K., Gell, P., 2001. The enigma of a late Pleistocene wetland in the Flinders Ranges, South Australia. *Quaternary International* 83–85, 129–144.
- Zhou, L., Williams, M., Peterson, J.A., 1994. Late Quaternary aeolianites, paleosols and depositional environments on the Nepean Peninsula, Victoria, Australia. *Quaternary Science Reviews* 13, 225–239.